HHS Public Access

Author manuscript

Biomol NMR Assign. Author manuscript; available in PMC 2023 August 02.

Published in final edited form as:

Biomol NMR Assign. 2022 October ; 16(2): 273–279. doi:10.1007/s12104-022-10091-6.

NMR resonance assignments of the DNA binding domain of mouse Junctophilin-2

Liping Yu[1,2], **Duane D. Hall**[3], **Weiyang Zhao**[3], **Long-Sheng Song**[1,3,4,5]

[1]Department of Biochemistry and Molecular Biology, Carver College of Medicine, University of Iowa, B291, CBRB, 285 Newton Road, Iowa City, IA 52242, USA

[2]CCOM NMR Core Facility, Carver College of Medicine, University of Iowa, Iowa City, IA 52242, USA

[3]Department of Internal Medicine, Carver College of Medicine, University of Iowa, 285 Newton Road, Iowa City, IA 52242, USA

[4]Fraternal Order of Eagles Diabetes Research Center, Carver College of Medicine, University of Iowa, Iowa City, IA 52242, USA

[5]Iowa City Veterans Affairs Medical Center, Iowa City, IA 52242, USA

Abstract

Junctophilin-2 (JP2) is a critical structural protein in the heart by stabilizing junctional membrane complexes between the plasma membrane and sarcoplasmic reticula responsible for precise Ca^{2+} regulation. Such complexes are essential for efficient cardiomyocyte contraction and adaptation to altered cardiac workload conditions. Mutations in the *JPH2* gene that encodes JP2 are associated with inherited cardiomyopathies and arrhythmias, and disruption of JP2 function is lethal. Interestingly, cardiac stress promotes the proteolytic cleavage of JP2 that triggers the translocation of its N-terminal fragment into the nucleus to repress maladaptive gene transcription. We previously found that the central region of JP2 is responsible for mediating direct DNA binding interactions. Recent structural studies indicate that this region serves as a structural role in the cytosolic form of JP2 by folding into a single continuous α-helix. However, the structural basis of how this DNA-binding domain interacts with DNA is not known. Here, we report the backbone and sidechain assignments of the DNA-binding domain (residues 331–413) of mouse JP2. These assignments reveal that the JP2 DNA binding domain is an intrinsically disordered protein and contains two α-helices located in the C-terminal portion of the protein. Moreover, this protein binds to DNA in a similar manner to that shown previously by electrophoretic mobility shift assays. Therefore, these assignments provide a framework for further structural studies into the interaction of this JP2 domain with DNA for the elucidation of transcriptional regulation of stress-responsive genes as well as its role in the stabilization of junctional membrane complexes.

✉Liping Yu, liping-yu@uiowa.edu, Long-Sheng Song, long-sheng-song@uiowa.edu.

Author contributions LY performed all the NMR analyses; DH and WZ prepared the samples; LY and DH drafted paper; LS secured funding and managed the project; All authors reviewed and edited the manuscript.

Competing interest The authors declare that they have no conflicts of interest.

Ethics approval and consent to participate All of our experiments comply with accepted ethical standards.

Consent for publication We agree to publish this paper.

Keywords

Junctophilin-2; Junctophilin; DNA binding; Cardiomyocyte; Excitation–contraction coupling; Cardiomyopathies

Biological context

The *JPH2* gene encodes Junctophilin-2 (JP2), a junctophilin family member that is essential for heart development (Chen et al. 2013; Reynolds et al. 2013; Takeshima et al. 2000), cardiomyocyte ultrastructural integrity and normal function (Guo et al. 2014; Landstrom et al. 2011; van Oort et al. 2011; Wei et al. 2010; Zhang et al. 2014). Mutations in JP2 are associated with hypertrophic and dilated cardiomyopathy and atrial arrhythmias (Beavers et al. 2013; Landstrom et al. 2007; Quick et al. 2017; Vanninen et al. 2018). Dysregulation of JP2 is considered an important factor in the pathogenesis of heart disease (Guo et al. 2014; Wang et al. 2018; Wei et al. 2010; Zhang et al. 2014). In mammals, there are four junctophilin genes that are expressed in a tissue-selective manner with JP2 primarily expressed in striated and smooth muscle (Calpena et al. 2018; Garbino et al. 2009; Landstrom et al. 2011; Takeshima et al. 2000). It is now appreciated that junctophilins function to facilitate physiologically relevant Ca^{2+} crosstalk by stabilizing narrow junctional contacts between the plasma membrane (PM) and endo/sarcoplasmic reticula (ER/SR). PM Ca^{2+} influx channels within these contacts are positioned near ER/SR Ca^{2+} efflux channels in excitable cells and near stromal interaction molecule (STIM) Ca^{2+} sensing proteins in most cell types (Chang et al. 2017; Takeshima et al. 2015). This subcellular configuration is responsible for such processes as Ca^{2+}-induced Ca^{2+} release and excitation–contraction coupling in muscle (Beavers et al. 2014; Chen et al. 2013; Corona et al. 2010), neuronal hyperpolarization and plasticity (Kakizawa et al. 2007; Moriguchi et al. 2006; Nishi et al. 2002; Sahu et al. 2019), insulin secretion in pancreatic beta cells (Li et al. 2016), and store-operated Ca^{2+} entry in immune cells (Woo et al. 2016). In cardiomyocytes, JP2 is required for stabilizing the integrity of the T-tubule membrane network essential for normal Ca^{2+} homeostasis and excitation–contraction coupling in stressed heart (Guo et al. 2014; Wang et al. 2018; Wei et al. 2010; Zhang et al. 2014).

Recently, we found that the N-terminal fragment of JP2 (called JP2NT, mouse $JP2^{1-565}$) produced by Ca^{2+}-dependent calpain cleavage in response to cardiac stress (Guo et al. 2015; Murphy et al. 2013; Wu et al. 2014) translocates to the nucleus and acts as a transcriptional repressor of stress-responsive genes (Guo et al. 2018). Deletion mutagenesis revealed that a $JP2NT^{\Delta 331-405}$ construct localizes to the nucleus but fails to co-purify with chromatin, indicating loss of DNA binding. We further demonstrated that a GST-$JP2^{331-405}$ fusion protein is sufficient for mediating direct DNA interactions by electrophoretic mobility shift assays. Initial sequence analysis and modeling suggested that residues ~ 350 to 420 of human JP2, corresponding to mouse $JP2^{343-413}$, is a putative α-helical region that may be important in determining PM–ER/SR gap distance (Garbino et al. 2009; Gross et al. 2020; Nishi et al. 2000). Recently, crystal structures of the JP1 and JP2 N-termini were solved, revealing that human JP1 residues 351–413 and human JP2 residues 362–423 do form a

single long α-helix that packs tightly against the tandem 8 MORN repeat array responsible for cytosolic $Ca_v1.1$ ion channel interactions (Yang et al. 2022).

Although JP2 is critical for cardiac function, presently there are no structural studies reported for any of the junctophilin homologs or their domains with regard to their interaction with DNA. Given that $JP2^{331–413}$ (mouse residues) is proposed to serve as both a structural "backbone" at PM–ER/SR junctions and a DNA binding domain in the nucleus, NMR assignments for this domain is a first step in understanding its contribution in transcriptional regulation.

Methods and experiments

Cloning, protein expression, and purification

A larger fragment of murine JP2 (amino acids 284–413) containing MORN domains 7 and 8 in addition to its DNA binding region was first cloned from pCMV6-XL5-JP2NTHA (Guo et al. 2018) and inserted into NheI and EcoRI digested pET28a. PCR was performed with Phusion DNA polymerase and 1× GC Buffer (New England Biolabs, Ipswitch, MA, USA) and oligonucleotides (Integrated DNA Techonolgies, Coralville, IA, USA) that incorporated NheI and TEV protease cleavage sites on the 5′ end and StrepTag II affinity tag and EcoRI sequences on the 3′ end. The sequence of the forward primer was 5′-ATG GCT AGC GAG AAC CTG TAC TTC CAA GGT ACC TAC ATG GGC GAG TGG-3′ and the reverse primer was 5′-CTC GAA TTC TCA TTT TTC GAA CTG CGG GTG GCT CCA GGC CAA TGT ACG GGC GAT G-3′. To obtain the $JP2^{331–413}$ expression vector, irrelevant sequences were removed using the QuikChange Lightening Mutagenesis kit (Agilent, Santa Clara, CA, USA). The pET28a thrombin sequence and the TEV and MORN domain insert sequences were deleted using sense (5′-CAT CAC AGC AGC GGC GAG GAG GGC AAG TAC-3′) and antisense (5′-GTA CTT GCC CTC CTC GCC GCT GCT GTG ATG-3′) oligos. Sanger sequencing confirmed that DNA isolated from candidate clones contained the expected N-terminal 6xHis tag (13 residues, MGSSHHHHHHSSG), mouse $JP2^{331–413}$ insert (83 residues), and C-terminal StrepTag II (8 residues, WSHPQFEK) with a total construct length of 104 residues.

The doubly tagged mouse JP2 DNA binding domain was expressed in BL21 (DE3) *Escherichia coli* (ThermoFisher Scientific). Cells were maintained on minimal media plates containing 6.8 g/L Na_2HPO_4, 3 g/L KH_2PO_4, 8.6 mM NaCl, 1.2 mM $MgSO_4$, 120 μM $CaCl_2$, 1 g/L NH_4Cl, 1 g/L glucose, 18 μM thiamine-HCl, 3 μg/mL $FeSO_4$, 1:1000 diluted trace metal mix A5 (Sigma, St. Louis, MO, USA), and 50 μg/mL kanamycin. To obtain uniformly ^{15}N- and ^{13}C-labeled protein, BL21 (DE3) cells were grown in the same media except with $^{15}NH_4Cl$ and $^{13}C_6$-glucose. Cultures (50 mL) were grown at 37 °C overnight and diluted to 0.05 OD_{600} in 1L prewarmed media and grown at 37 °C until OD_{600} reached ~ 0.8–1.0. JP2 protein expression was induced with 250 μM IPTG at room temperature for three hours which gave maximal expression. Cultures were then pelleted by centrifugation (6000×*g*, 20 min, 4 °C) and cell pellets frozen at − 80 °C. The harvested cells were then thawed and lysed in 100 mL Buffer A [20 mM Tris pH 8.0, 150 mM NaCl, 1 mM DTT and Mini cOmplete protease inhibitors (Roche Applied Science, Indianapolis, IN, USA)] supplemented with 100 μg/mL lysozyme (Research Products International, Mount Prospect,

IL, USA), 25 U/mL Benzonase (EMD Millipore, Burlington, MA, USA) and 2 mg/mL $MgCl_2$ and incubated at 37 °C for 30 min. Lysates were chilled on ice for 20 min before sonication on ice (10 mL batches, four 15 s pulses each) and centrifugation (20,000×*g*, 20 min, 4 °C). The cleared supernatant (SN1) was saved and the pellet was solubilized in 20 mL of Buffer A with 1% Triton X-100, 0.5% Na-deoxycholate and 0.1% SDS, centrifuged (20,000×*g*, 20 min, 4 °C), and resulted in the second supernatant (SN2). Coomassie-stained gels revealed that the soluble SN1 fraction contained ~ 80% of JP2 DNA-binding domain protein when compared to SN2 fraction.

The doubly tagged (N-terminal His tag + C-terminal Strep tag) and $^{15}N/^{13}C$-labeled mouse JP2 DNA binding domain was then affinity-purified first over StrepTactin XT resin (IBA Life Sciences, Goettingen, Germany) from SN1 and fivefold diluted SN2 in Buffer A. The loaded column was then washed first using high salt buffer (20 mM Tris pH 8.0, 500 mM NaCl) followed by low salt Buffer W (20 mM Tris pH 8.0, 150 mM NaCl). The bound JP2 protein was then eluted with 50 mM Tris, 150 mM NaCl and 50 mM biotin (IBA Life Sciences) at pH 8.0. Biotin eluates were diluted five-fold in Buffer W and subjected to a second purification by binding to His-select columns (Sigma), washing with Buffer W, and eluting with a buffer containing 50 mM Tris, 150 mM NaCl, and 250 mM imidazole at pH 8.0. The JP2 protein purified from the double affinity purifications was shown to be highly pure by Coomassie-stained gels. Amicon Ultra centrifugal filters (3000 MWCO, EMD Millipore) were used for protein concentration and buffer exchange into an NMR buffer composed of 20 mM BisTris, 40 mM NaCl, and pH 6.0 for NMR studies.

NMR spectroscopy

NMR spectra were acquired on a Bruker Avance Neo 600 MHz NMR spectrometer at 20 °C using 0.8 mM uniformly [^{13}C,^{15}N]-labeled mouse JP2 DNA binding domain in a buffer composed of 20 mM BisTris, 40 mM NaCl, and pH 6.0 in 90% H_2O/10% D_2O. A suite of triple resonance NMR experiments including HNCACB, CBCA(CO)NH, HNCO, HN(CA)CO, HNCA, and HN(CO)CA experiments (Yamazaki et al. 1994) were collected for backbone assignments of JP2 DNA binding domain. Side-chain assignments were obtained by acquiring C(CO)NH, H(CCO) NH, and HBHA(CO)NH experiments (Clore and Gronenborn 1994). All the triple resonance experiments were acquired in NUS format as previously described (Hyberts et al. 2012; Robson et al. 2019). The collected NMR data were processed using NMRPipe (Delaglio et al. 1995) and SMILE (Ying et al. 2017), and analyzed using NMRView (Johnson and Blevins 1994).

Extent of assignments and data deposition

The $^{15}N/^{1}H$ HSQC spectrum of JP2 DNA binding domain is shown in Fig. 1. Clearly, the cross-peaks in the HSQC spectrum are not well dispersed as typically observed for a well folded protein. Instead, the cross-peaks are clustered in a narrow strip with the backbone amide NH protons resonated in a narrow ^{1}H range from 7.89 to 8.73 ppm, indicating that this JP2 domain is an intrinsically disordered protein (IDP). All backbone amide cross-peaks in the $^{15}N/^{1}H$ HSQC spectrum of JP2 DNA binding domain are assigned and labeled using the wild type protein sequence numbering (Fig. 1). It is noted that our protein construct contains an N-terminal 6xHis-tag (MGSSHHHHHHSSG, 13 residues numbered as 318 to

330), mouse JP2 DNA-binding domain (residues 331 to 413), and a C-terminal Strep tag II (WSHPQFEK, 8 residues numbered as 414 to 421). Therefore, excluding the His-tag (13 residues) at the N-terminus, 100% (89 out of 89) of non-proline backbone amides, 100% (91 out of 91) of Cα, Cβ, and CO, and 97% (88 out of 91) of Hα are assigned. Moreover, more than 97% of the protein sidechain ^{1}H and ^{13}C resonances have been assigned except for the 7 aromatic rings. The assigned chemical shifts of JP2 DNA binding domain were deposited in BioMagResBank (https://bmrb.io) under the accession number 51405.

Figure 2 shows the plots of predicted probability of α-helical and β-sheet secondary structures and predicated random coil index (RCI) order parameter (S^2) as a function of residue number of the mouse JP2 DNA binding domain. The secondary structures of the JP2 DNA binding domain obtained from the analysis of the assigned backbone atoms (H_N, N, Cα, Cβ, CO, Hα) using TALOS + (Shen et al. 2009) are labeled (Fig. 2). Clearly, the JP2 DNA binding domain contains two α-helices located in the C-terminal half of the protein. β-sheet secondary structures were not detected, except for two β-sheet-like residues L340 and V348 in the N-terminal part of the protein. Moreover, the two helical regions of the protein are more ordered than the rest of the protein, since only the two α-helices exhibit RCI order parameter S^2 in the range of 0.7–0.8, while the rest of the protein have S^2 near or below 0.5.

Figure 3 shows the plot of consensus chemical shift index (CSI) as a function of residue number of the mouse JP2 DNA binding domain. Consensus CSI calculated from the backbone assignments has been widely used to determine protein secondary structures (Hafsa and Wishart 2014). In a typical CSI plot, α-helices give a negative CSI of − 1, while β-sheets have a positive CSI of + 1 (Hafsa and Wishart 2014). CSI analysis of our assigned JP2 DNA binding domain indicates that there are two α-helices in this protein, consistent with the results from the TALOS + analysis. However, CSI suggests that the α1 helix is slightly longer with two extra helical residues at its N-terminal end, when compared to the results from TALOS + analysis. Furthermore, CSI also indicates that there are no β-sheets present in this protein.

Electrophoretic mobility shift assay previously demonstrated that this region of JP2 binds to DNA (Guo et al. 2018). Therefore, with these assignments, we will start in the next studies to investigate how this JP2 domain interacts with DNA to regulate transcription of stress-responsive genes. The secondary structure that we have determined here for the mouse JP2 DNA binding domain in solution differs from the one observed in the crystal structures of human JP1 and JP2 N-terminal MORN-helical domain (Yang et al. 2022) where this region forms a single long α-helix. When expressed as part of a larger protein including the eight N-terminal MORN repeats of human Junctophilins, residues equivalent to mouse 331–413 may favor a single extended α-helix and be stabilized by interacting with the MORN repeat array. In contrast, residues 331–413 of mouse JP2 are more intrinsically disordered in isolation and in solution where two smaller α-helical segments remain within its C-terminal end. It is the goal of our future work to determine how this domain rearranges upon binding with its DNA target sequence.

Acknowledgements

This work was supported by the Albaghdadi Family Foundation and NHLBI (R01 HL130346). We also acknowledge the personnel and instrumentation in the University of Iowa Carver College of Medicine NMR Facility, supported by the Roy J. and Lucille A. Carver College of Medicine and grants from the Roy J. Carver Charitable Trust.

Funding

This work was supported by the Albaghdadi Family Foundation and NHLBI (R01 HL130346). The 800 MHz NMR spectrometer was funded by Roy J. Carver Charitable Trust of Roy J. and Lucille A. Carver College of Medicine, and the 600 MHz NMR spectrometer was funded by the University of Iowa Roy J. and Lucille A. Carver College of Medicine.

Data availability

The chemical shift values have been deposited in BioMagResBank (https://bmrb.io) under the Accession Number 51405.

References

Beavers DL et al. (2013) Mutation E169K in junctophilin-2 causes atrial fibrillation due to impaired RyR2 stabilization. J Am Coll Cardiol 62:2010–2019. 10.1016/j.jacc.2013.06.052 [PubMed: 23973696]

Beavers DL, Landstrom AP, Chiang DY, Wehrens XH (2014) Emerging roles of junctophilin-2 in the heart and implications for cardiac diseases. Cardiovasc Res 103:198–205. 10.1093/cvr/cvu151 [PubMed: 24935431]

Calpena E, Lopez Del Amo V, Chakraborty M, Llamusi B, Artero R, Espinos C, Galindo MI (2018) The *Drosophila* junctophilin gene is functionally equivalent to its four mammalian counterparts and is a modifier of a Huntingtin poly-Q expansion and the Notch pathway. Dis Model Mech. 10.1242/dmm.029082

Chang CL, Chen YJ, Liou J (2017) ER-plasma membrane junctions: why and how do we study them? Biochim Biophys Acta Mol Cell Res 1864:1494–1506. 10.1016/j.bbamcr.2017.05.018 [PubMed: 28554772]

Chen B et al. (2013) Critical roles of junctophilin-2 in T-tubule and excitation-contraction coupling maturation during postnatal development. Cardiovasc Res 100:54–62. 10.1093/cvr/cvt180 [PubMed: 23860812]

Clore GM, Gronenborn AM (1994) Multidimensional heteronuclear nuclear magnetic resonance of proteins. Methods Enzymol 239:349–363 [PubMed: 7830590]

Corona BT, Balog EM, Doyle JA, Rupp JC, Luke RC, Ingalls CP (2010) Junctophilin damage contributes to early strength deficits and EC coupling failure after eccentric contractions. Am J Physiol Cell Physiol 298:C365–376. 10.1152/ajpcell.00365.2009 [PubMed: 19940065]

Delaglio F, Grzesiek S, Vuister GW, Zhu G, Pfeifer J, Bax A (1995) NMRPipe: a multidimensional spectral processing system based on UNIX pipes. J Biomol NMR 6:277–293 [PubMed: 8520220]

Garbino A, van Oort RJ, Dixit SS, Landstrom AP, Ackerman MJ, Wehrens XH (2009) Molecular evolution of the junctophilin gene family. Physiol Genomics 37:175–186. 10.1152/physiolgenomics.00017.2009 [PubMed: 19318539]

Gross P et al. (2020) Interaction of the joining region in junctophilin-2 with the L-type Ca(2+) channel is pivotal for cardiac dyad assembly and intracellular Ca(2+) dynamics. Circ Res. 10.1161/CIRCRESAHA.119.315715

Guo A et al. (2014) Overexpression of junctophilin-2 does not enhance baseline function but attenuates heart failure development after cardiac stress. Proc Natl Acad Sci USA 111:12240–12245. 10.1073/pnas.1412729111 [PubMed: 25092313]

Guo A et al. (2015) Molecular determinants of calpain-dependent cleavage of junctophilin-2 protein in cardiomyocytes. J Biol Chem 290:17946–17955. 10.1074/jbc.M115.652396 [PubMed: 26063807]

Guo A et al. (2018) E-C coupling structural protein junctophilin-2 encodes a stress-adaptive transcription regulator. Science. 10.1126/science.aan3303

Hafsa NE, Wishart DS (2014) CSI 2.0: a significantly improved version of the Chemical Shift Index. J Biomol NMR 60:131–146. 10.1007/s10858-014-9863-x [PubMed: 25273503]

Hyberts SG, Milbradt AG, Wagner AB, Arthanari H, Wagner G (2012) Application of iterative soft thresholding for fast reconstruction of NMR data non-uniformly sampled with multidimensional Poisson Gap scheduling. J Biomol NMR 52:315–327. 10.1007/s10858-012-9611-z [PubMed: 22331404]

Johnson BA, Blevins RA (1994) NMR View: A computer program for the visualization and analysis of NMR data. J Biomol NMR 4:603–614. 10.1007/BF00404272 [PubMed: 22911360]

Kakizawa S et al. (2007) Junctophilin-mediated channel crosstalk essential for cerebellar synaptic plasticity. EMBO J 26:1924–1933. 10.1038/sj.emboj.7601639 [PubMed: 17347645]

Landstrom AP et al. (2007) Mutations in JPH2-encoded junctophilin-2 associated with hypertrophic cardiomyopathy in humans. J Mol Cell Cardiol 42:1026–1035. 10.1016/j.yjmcc.2007.04.006 [PubMed: 17509612]

Landstrom AP et al. (2011) Junctophilin-2 expression silencing causes cardiocyte hypertrophy and abnormal intracellular calcium-handling. Circ Heart Fail 4:214–223. 10.1161/CIRCHEARTFAILURE.110.958694 [PubMed: 21216834]

Li L et al. (2016) Junctophilin 3 expresses in pancreatic beta cells and is required for glucose-stimulated insulin secretion. Cell Death Dis 7:e2275. 10.1038/cddis.2016.179 [PubMed: 27336719]

Moriguchi S et al. (2006) Functional uncoupling between Ca2+ release and afterhyperpolarization in mutant hippocampal neurons lacking junctophilins. Proc Natl Acad Sci USA 103:10811–10816. 10.1073/pnas.0509863103 [PubMed: 16809425]

Murphy RM, Dutka TL, Horvath D, Bell JR, Delbridge LM, Lamb GD (2013) Ca2+-dependent proteolysis of junctophilin-1 and junctophilin-2 in skeletal and cardiac muscle. J Physiol 591:719–729. 10.1113/jphysiol.2012.243279 [PubMed: 23148318]

Nishi M, Mizushima A, Nakagawara K, Takeshima H (2000) Characterization of human junctophilin subtype genes. Biochem Biophys Res Commun 273:920–927. 10.1006/bbrc.2000.3011 [PubMed: 10891348]

Nishi M, Hashimoto K, Kuriyama K, Komazaki S, Kano M, Shibata S, Takeshima H (2002) Motor discoordination in mutant mice lacking junctophilin type 3. Biochem Biophys Res Commun 292:318–324. 10.1006/bbrc.2002.6649 [PubMed: 11906164]

Quick AP et al. (2017) Novel junctophilin-2 mutation A405S is associated with basal septal hypertrophy and diastolic dysfunction. JACC Basic Transl Sci 2:56–67. 10.1016/j.jacbts.2016.11.004 [PubMed: 28393127]

Reynolds JO et al. (2013) Junctophilin-2 is necessary for T-tubule maturation during mouse heart development. Cardiovasc Res 100:44–53. 10.1093/cvr/cvt133 [PubMed: 23715556]

Robson S, Arthanari H, Hyberts SG, Wagner G (2019) Chapter Ten: nonuniform sampling for NMR spectroscopy. In: Wand AJ (ed) Methods in enzymology, vol 614. Academic Press, Cambridge, pp 263–291 [PubMed: 30611427]

Sahu G, Wazen RM, Colarusso P, Chen SRW, Zamponi GW, Turner RW (2019) Junctophilin proteins tether a Cav1-RyR2-KCa3.1 tripartite complex to regulate neuronal excitability. Cell Rep 28:2427–2442 e2426. 10.1016/j.celrep.2019.07.075 [PubMed: 31461656]

Shen Y, Delaglio F, Cornilescu G, Bax A (2009) TALOS+: a hybrid method for predicting protein backbone torsion angles from NMR chemical shifts. J Biomol NMR 44:213–223. 10.1007/s10858-009-9333-z [PubMed: 19548092]

Takeshima H, Komazaki S, Nishi M, Iino M, Kangawa K (2000) Junctophilins: a novel family of junctional membrane complex proteins. Mol Cell 6:11–22. 10.1016/s1097-2765(00)00003-4 [PubMed: 10949023]

Takeshima H, Hoshijima M, Song LS (2015) Ca(2)(+) microdomains organized by junctophilins. Cell Calcium 58:349–356. 10.1016/j.ceca.2015.01.007 [PubMed: 25659516]

van Oort RJ et al. (2011) Disrupted junctional membrane complexes and hyperactive ryanodine receptors after acute junctophilin knockdown in mice. Circulation 123:979–988. 10.1161/CIRCULATIONAHA.110.006437 [PubMed: 21339484]

Vanninen SUM et al. (2018) Heterozygous junctophilin-2 (JPH2) p.(Thr161Lys) is a monogenic cause for HCM with heart failure. PLoS ONE 13:e0203422. 10.1371/journal.pone.0203422

Wang Y et al. (2018) Targeting calpain for heart failure therapy: implications from multiple murine models. JACC Basic Transl Sci 3:503–517. 10.1016/j.jacbts.2018.05.004 [PubMed: 30175274]

Wei S et al. (2010) T-tubule remodeling during transition from hypertrophy to heart failure. Circ Res 107:520–531. 10.1161/CIRCRESAHA.109.212324 [PubMed: 20576937]

Woo JS, Srikanth S, Nishi M, Ping P, Takeshima H, Gwack Y (2016) Junctophilin-4, a component of the endoplasmic reticulumplasma membrane junctions, regulates Ca2+ dynamics in T cells. Proc Natl Acad Sci USA 113:2762–2767. 10.1073/pnas.1524229113 [PubMed: 26929330]

Wu CY et al. (2014) Calpain-dependent cleavage of junctophilin-2 and T-tubule remodeling in a mouse model of reversible heart failure. J Am Heart Assoc 3:e000527. 10.1161/JAHA.113.000527

Yamazaki T, Lee W, Arrowsmith CH, Muhandiram DR, Kay LE (1994) A suite of triple-resonance NMR experiments for the backbone assignment of 15N, 13C, 2H-labeled proteins with high sensitivity. J Am Chem Soc 116:11655–11666

Yang ZF, Panwar P, McFarlane CR, Tuinte WE, Campiglio M, Petegem FV (2022) Structures of the junctophilin/voltage-gated calcium channel interface reveal hot spot for cardiomyopathy mutations. Proc Natl Acad Sci USA 119:e2120416119. 10.1073/pnas.2120416119

Ying J, Delaglio F, Torchia DA, Bax A (2017) Sparse multidimensional iterative lineshape-enhanced (SMILE) reconstruction of both non-uniformly sampled and conventional NMR data. J Biomol NMR 68:101–118. 10.1007/s10858-016-0072-7 [PubMed: 27866371]

Zhang C et al. (2014) Microtubule-mediated defects in junctophilin-2 trafficking contribute to myocyte transverse-tubule remodeling and Ca2+ handling dysfunction in heart failure. Circulation 129:1742–1750. 10.1161/CIRCULATIONAHA.113.008452 [PubMed: 24519927]

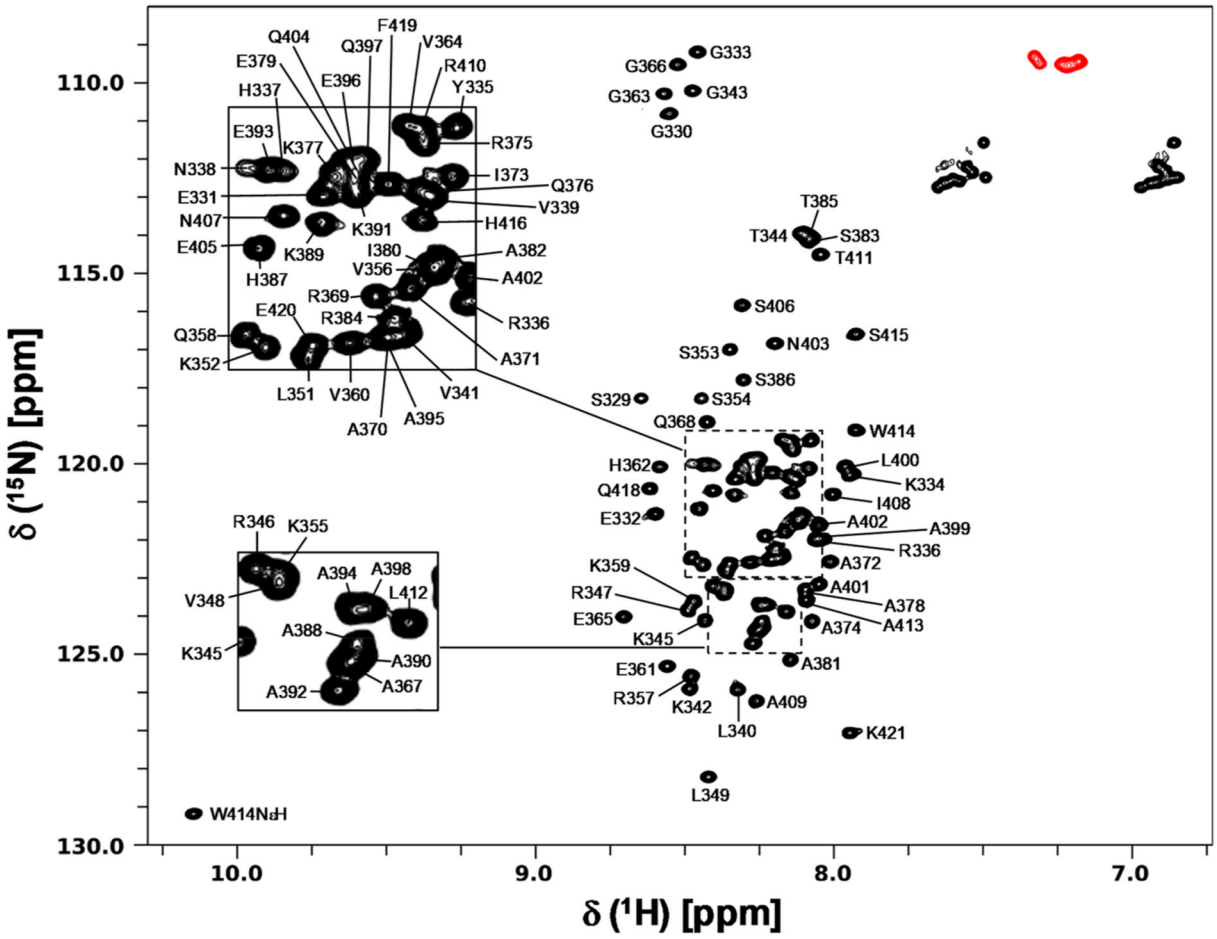

Fig. 1.

$^{15}N/^{1}H$ HSQC spectrum of the mouse junctophilin-2 (JP2) DNA-binding domain. The assigned backbone amides are labeled using the wild-type protein sequence numbering. The N-terminal His-tag (13 residues) was numbered as 318 to 330, while the C-terminal Strep-tag II (8 residues) was numbered as 414 to 421. The folded peaks are colored in red. The insets show the peak labelling of two crowded regions as indicated by the dotted rectangular boxes

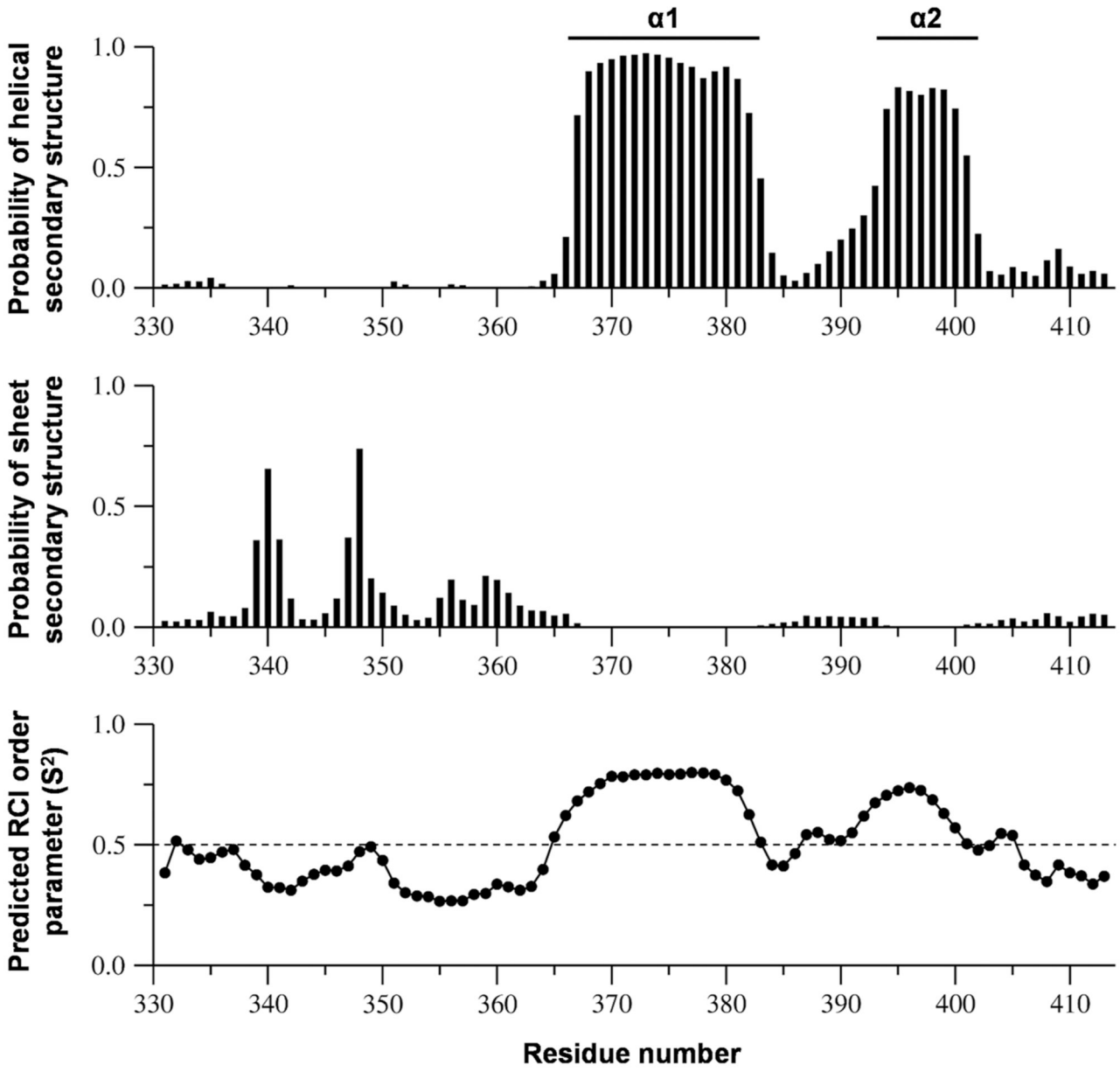

Fig. 2.

Plots of predicted probability of helical and sheet secondary structures and RCI order parameter (S^2) as a function of residue number of the mouse junctophilin-2 (JP2) DNA-binding domain. Wild-type protein sequence numbering is used here. These predicted probability values and RCI order parameters were obtained from the TALOS + analysis of the assigned backbone atoms (H_N, N, Cα, Cβ, CO, Hα). The secondary structures obtained from these analyses of the assigned backbone of JP2 are labeled in the figure

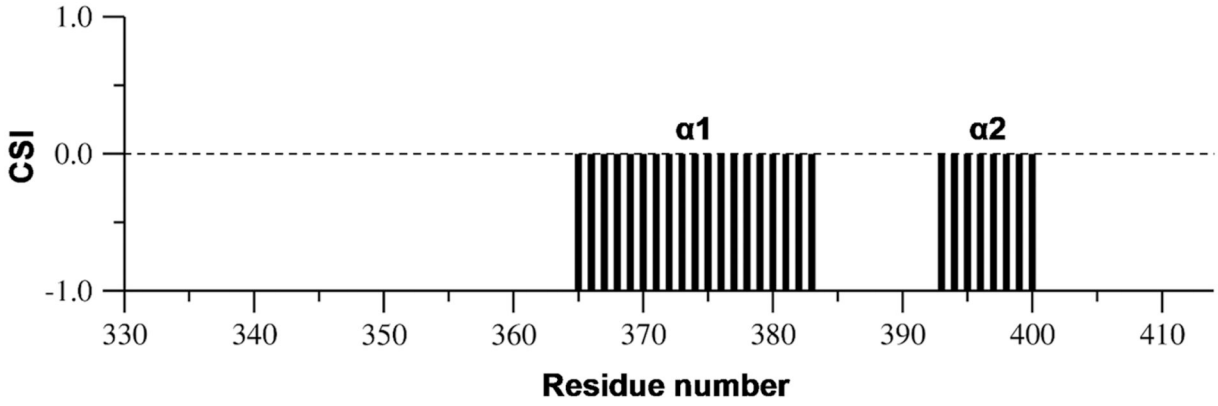

Fig. 3.

Plot of the consensus chemical shift index (CSI) as a function of residue number of the mouse junctophilin-2 (JP2) DNA-binding domain. Wildtype protein sequence numbering is used here. The consensus CSI values were obtained from the assigned backbone atoms by using the program CSI 2.0